Modal interaction and vibration suppression in industrial turbines using adjustable journal bearings

Athanasios Chasalevris[1] **and Fadi Dohnal**[2]

[1]GE Oil & Gas, Newbold Road, Rugby CV212NH, United Kingdom
[2]Lindenstrasse 13, 5430 Wettingen, Switzerland

[1]athanasios.chasalevris@ge.com

Abstract. The vibration suppression by deliberately introducing a parametric excitation in the fluid-film bearings is investigated for an industrial turbine rotor system. A journal bearing with variable adjustable geometry is operated in such a way that the effective stiffness and damping properties vary periodically in time. The proposed bearing is designed for having the ability of changing the bearing fluid film thickness in a semi-active manner. Such an adjustment of the journal bearing properties introduces in the system a time-periodic variation of the effective stiffness and damping properties of the fluid-film. If the time-periodicity is tuned properly to match a parametric anti-resonance, vibration suppression is achieved in the overall system. The paper presents the principle of operation of the recently developed bearings. The simulation of an industrial turbine rotor-bearing shaft line at induced parametric excitation motivates the further development and application of such bearings since the vibration amplitudes are considerably decreased in critical speeds.

1. Introduction

Several journal bearing initiatives have been launched on improving the rotordynamic efficiency of industrial turbines. The demands for vibration control in rotating machinery motivated the development and application of journal bearings with adjustable/controllable properties the latest 20 years. The reduction of vibration through the application of adjustable/controllable journal bearings has been proved to be beneficial for many kinds of rotating machinery. Through the concept of adjustable properties of journal bearings it is possible to increase the stability of the rotor-bearing system, to enlarge its operational frequency range, to suppress resonance vibration amplitude, to reposition journal centre of rotation whilst in operation, to suppress journal orbits for a range of loads, and to provide reduced oil temperature rises compared to the conventional bearing. Theoretical modelling and practical tests have demonstrated clear improvements over conventional fluid film bearings, along with a number of other characteristics offering benefits that may be of interest to designers and users of such bearings.

In general, several methods have been presented in order to dissipate the vibration energy and to keep low vibration levels in rotating machines. Among these mechanisms are seal dampers (Vance and Li, [1]), squeeze-film dampers (San Andres and Lubell [2]), hybrid squeeze-film dampers (El-Shafei and Hathout [3]), and magnetorheological squeeze-film dampers [4-7]. Mechanisms that incorporate active adjustment of journal bearing properties have been proposed since the last 20 years; among them the hydraulic active chamber systems (Ulbrich and Althaus [8], Althaus et al. [9, 10], and Santos [11]), and the variable impedance hydrodynamic journal bearings (Goodwin et al. [12]). The

magnetized journal bearings lubricated with ferro fluids (Osman et al. [13]) offer also the benefit of controlling the fluid film properties because of their controllability by an external magnetic force.

When part of the hydrostatic pressure is dynamically modified by means of hydraulic control systems, one refers to the active lubrication. The concepts of the actively lubricated bearings (Santos [14], Santos and Russo [15], Santos and Nicoletti [16], and Santos and Scalabrin [17]) and of the active-control on fluid bearings (Bently et al. [18]) have met also wide research and remains still under promising investigation. By the association of electronics, control design, and hydraulics, the active lubrication simultaneously allows the reduction of wear between rotating and nonrotating parts of the machinery and, in addition, the attenuation of rotor vibration. Recent theoretical (Santos and Nicoletti [19], and Nicoletti and Santos [20]) and experimental (Santos and Scalabrin [21]) investigations related to active lubrication showed the feasibility of attenuating rotor vibrations in test rigs with rigid rotors. The use of active lubrication in tilting-pad journal bearings (TPJB) has the strong advantage of resulting to bearings with negligible cross-coupling effects between orthogonal directions. However, this kind of active strategy can also be applied to hydrostatic (Bently et al. [16]) and to multilobed bearings (Santos et al. [21]).

On the concept of introducing the variable geometry of a journal bearing in order to adjust its properties there are several contributions with various methods for the adjustment of the clearances through the deformation of the bearing pads; among them a novel adjustable multi-lobe hydrodynamic journal bearing was designed, manufactured, fitted and experimentally tested by Martin and Parkins [22] and Martin [23] replacing a conventional bearing in a large marine gearbox. The novel bearing demonstrated the ability to suppress journal orbits and to translate the journal orbit in a controlled manner by an amount exceeding double the clearance of the conventional bearing. A novel tight-tolerance tilt-pad journal bearing that provides increased stability in high speed turbomachinery was analyzed and measured by Bischof and Zhou [24]. On a similar way, an active journal bearing with a flexible sleeve that is deformed under controlled pressure of a hydraulic chamber has been developed by Krodkiewski and Sun [25] and Krodkiewski [26] as a method to control the stability of rotor-bearing systems.

Unlike most of works of the past that incorporated various mechanisms for active control of bearing properties through the lubrication pressure or the bearing deformation (geometry), the present work introduces the technique of modal interaction through a recently developed partial arc journal bearing of adjustable geometry/properties [27]. The principle of parametric resonance and anti-resonance that has been extensively studied [28-31] was applied also recently in a Jeffcott rotor system mounted on AMBs [32]. The activation of coupling between two modes of vibration under specific periodic change of the bearing stiffness coefficients impacts the maximum amplitude developed during passage through resonance at a constant run-up. The principle is studied in this paper by implementing the periodic stiffness variation of the bearings by periodical changing of the fluid film bearing geometry [33-34] under a recently proposed bearing configuration [27]. This work aims to orient the application of such vibration suppression mechanism to industrial turbine applications and to investigate the efficiency and applicability considering actual stiffness and damping design characteristics of the system. The impact of modal interaction to the 1^{st} critical speed amplitude is presented on a Jeffcott rotor application of similar properties to those of a higher speed industrial turbine (>7000RPM) with the results to show even up to 70% amplitude reduction. At the last section, a turbine rotor of Rated speed higher than 7000RPM is simulated using the Transient Transfer Matrix Method (TTMM) [35] and the response amplitude is evaluated numerically as a function of rotating speed during a slow run-up of constant speed rate. With the rated speed to be in between 1^{st} and 2^{nd} critical speed the application of the method is shown to be very beneficial on reducing the 1^{st} critical amplitude under certain bearing stiffness and damping variation.

2. Implementing periodic stiffness and damping coefficients in journal bearings

The periodic variation of the stiffness and damping coefficients of the fluid film is implemented in this study using the proposed partial arc journal bearing shown in figure 1 [27]. The proposed journal bearing with variable geometry enables the periodic variation of its properties by displacing its pads with the desired frequency Ω_{ex} and at amplitude d_0 that is supposed to result in a respective variation of the stiffness and damping coefficient regarding the operating conditions. The domain of values of excitation frequency is expected not to exceed 10~15 times the 1st critical speed of the rotor, meaning that values up to 3000-3500rad/s are expected to be applicable for higher speed industrial turbines, e.g. Turbines running at a rated speed of 500-800rad/s regarding their size, after having passed through their 1st, existing usually between 200-300rad/s.

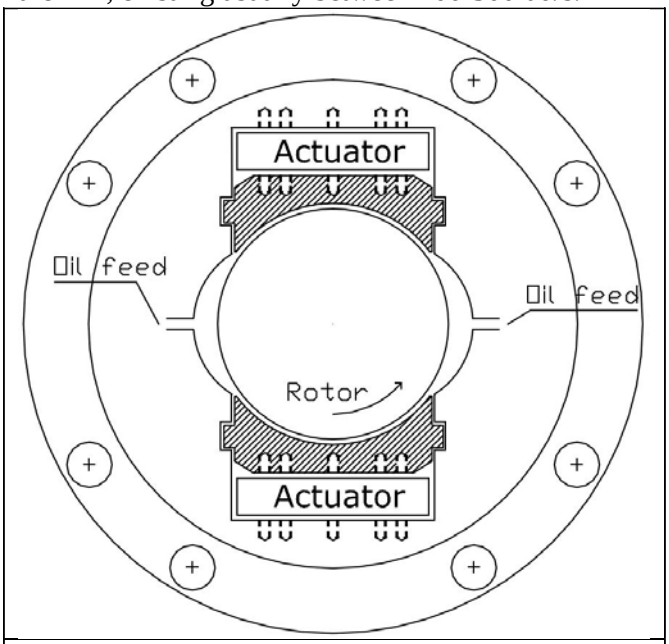

Figure 1. Representation of the principle of operation for the 2-arc bearing with variable geometry and adjustable properties [27]

Regarding the amplitude d_0 of the pad vibration, it should be expressed as a small percentage of bearing radial clearance, e.g. 1%-10% meaning that for an industrial turbine application, an absolute amplitude d_0 of 5-50μm should be expected in the application.

Regarding the loading conditions and the eccentricity of the journal at operation, the variation of the bearing properties should occur at a range of 10% to 50% of its nominal values. The amplitude ε of variation for K_{ij} and C_{ij} has not to be equal or similar.

As it is shown in figure 2, the higher the frequency of excitation Ω_{ex} and the amplitude d_0 are, the more the variation of stiffness coefficients is. Similar progress is noticed for the damping coefficients as well. The variation of the stiffness and damping properties has not to be strictly sinusoidal so as the principal of parametric excitation to be applicable; periodic variation is able to introduce the modal interaction into the vibrating system.

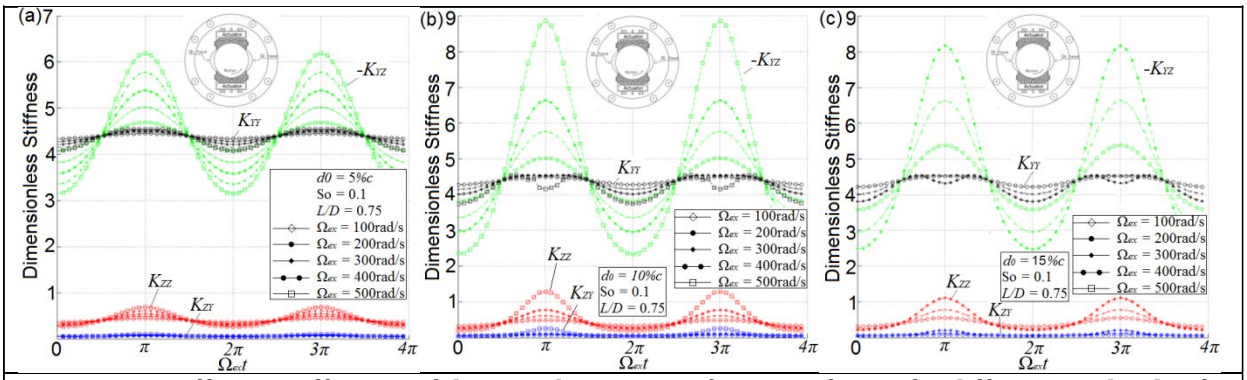

Figure 2. Stiffness coefficients of the 3-arc bearing as a function of time, for different amplitude of pad displacement a) $d_0 = 5\%c$, b) $d_0 = 10\%c$, and c) $d_0 = 15\%c$, variable cases of excitation frequency Ω_{ex}, and for $\mathrm{So} = 1$.

3. Introducing modal interaction in a Jeffcott rotor

The preliminary study of the modal interaction using variable bearing coefficients is presented in this section aiming to highlight the principal and the benefit of vibration suppression. In the next section 4 the application is extended to a realistic model of an industrial turbine for power generation. Assuming a Jeffcott rotor as in figure 3, carrying a disc of mass m_d at its mid-span and two rotor studs of mass m_j at its ends, mounted in two journal bearings of linear coefficients, the motion equations are written as in equation (1) with the bearing impedance forces to be implemented as in equation (2). In equations (1) and (2), y and z are the vertical and horizontal displacements of the disc, while y_j and z_j are the vertical and horizontal displacements of the journals that are assumed to be equal in both journals due to the symmetry of the system. The rotor experiences uniformly accelerated rotation of low magnitude with $\dot{\Omega} = 5\text{rad/s}^2$ and $\dot{\Omega}/\Omega_0^2 \approx 8.68e-5$, where Ω_0 is defined in table 1 together with the basic geometrical and physical properties of the system, that is supposed to correspond to an industrial steam turbine application of higher speed . The disc is supposed to execute a whirling due to the deformation of the elastic rotor with very small amplitude $\delta = \left(y^2 + z^2\right)^{1/2}$ (see figure 3) compared to rotor's length, thus in equation (1) the components related to tangential acceleration $\dot{\Omega}\cdot\delta$ are neglected.

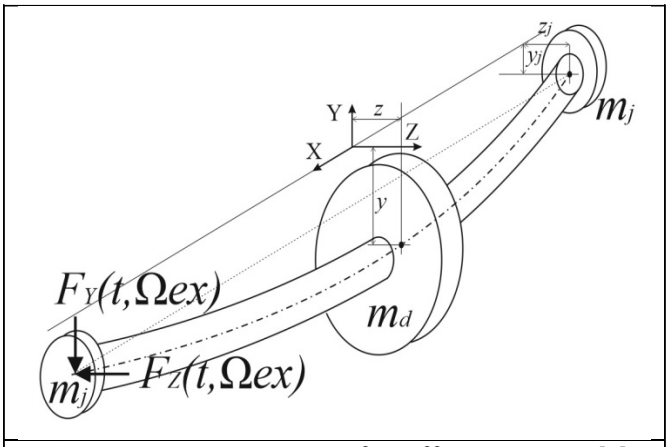

Figure 3. Representation of a Jeffcott rotor model carrying two masses at its ends [34]

$$\begin{aligned} m_d\ddot{y} + K\left(y - y_j\right) &= -m_d\,\delta\,\Omega^2 \sin\left(\dot{\Omega}t^2/2\right) \\ m_d\ddot{z} + K\left(z - z_j\right) &= m_d\,\delta\,\Omega^2 \cos\left(\dot{\Omega}t^2/2\right) \\ -2m_j\ddot{y}_j + K\left(y - y_j\right) - 2F_Y &= 0 \\ -2m_j\ddot{z}_j + K\left(z - z_j\right) - 2F_Z &= 0 \end{aligned} \tag{1}$$

$$\begin{aligned} F_Y &= K_{YY}y_j + C_{YY}\dot{y}_j + K_{YZ}z_j + C_{YZ}\dot{z}_j \\ F_Z &= K_{ZZ}z_j + C_{ZZ}\dot{z}_j + K_{ZY}y_j + C_{ZY}\dot{y}_j \end{aligned} \tag{2}$$

This very simplistic model aims to correspond in vibration amplitude and natural frequency to the realistic example following in section 4. As it is seen in equation (1), the discs are not modelled for tilting motions but only for lateral displacement, so although the 1st mode would correspond to a realistic example, the 2nd mode would not do. The journal masses are mounted at the ends of Jeffcott rotor so as to introduce the 2nd natural mode that would maximize the relative vibration of the ends of the rotor with respect to the mid-span displacement. Under this consideration, the system will show that the modal interaction occurs in specific frequencies of bearing coefficient variation and deducts energy from the 1st mode (less damped) to transfer it at the 2nd mode (much damped) and in this way to decrease the vibration amplitude when the system vibrates at 1st mode (1st critical speed).

The only source of damping is the fluid film viscous damping expressed with realistic values in table 1. Bearing stiffness coefficients correspond also approximately to a real application. The ratio of rotor stiffness to bearing stiffness has been also considered to meet realistic examples. Pedestal properties are not incorporated in this study in order to focus on the rotor-bearing interaction and they are left to be presented in upcoming works. Unbalance magnitude corresponds to the permissible residual unbalance defined by GE standards.

Table 1. Basic geometrical and physical properties of the Jeffcott rotor

Rotor		Bearing
Disc Mass	$m_d = 5000\text{kg}$	$\begin{bmatrix} K_{YY} & K_{YZ} \\ K_{ZY} & K_{ZZ} \end{bmatrix} = K \begin{bmatrix} 1.5 & -10 \\ -1 & 7 \end{bmatrix}$, N/m
Journal Mass	$m_j = 500\text{kg}$	
Slenderness ratio	$L/D \approx 9$	$\begin{bmatrix} C_{YY} & C_{YZ} \\ C_{ZY} & C_{ZZ} \end{bmatrix} = 10^5 \begin{bmatrix} 60 & -19 \\ -15 & 8 \end{bmatrix}$, Ns/m
Young Modulus	$E = 210\text{GPa}$	
1st natural freq.	$\Omega_0 \approx 240\text{rad/s}$	
Stiffness	$K = 48EI / L^3$	

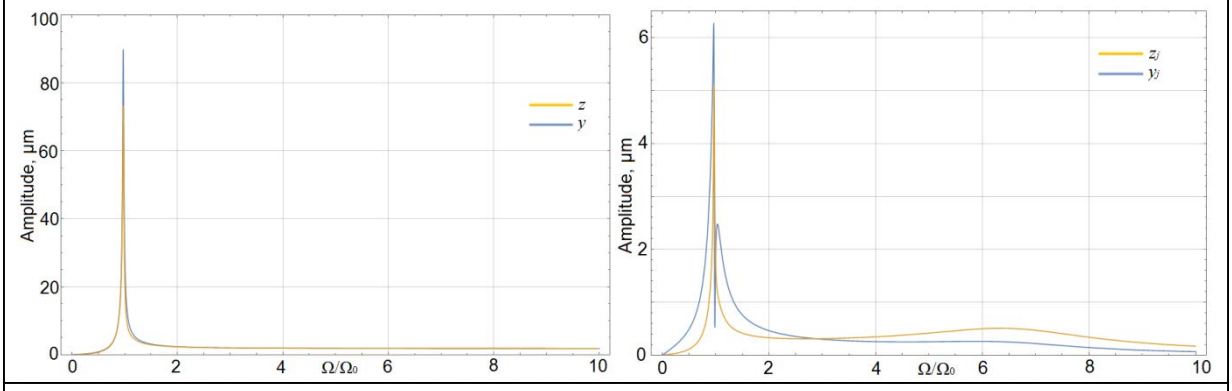

Figure 4. Disc (left) and journals (right) 0-pk amplitude as a function of rotating speed, solved analytically

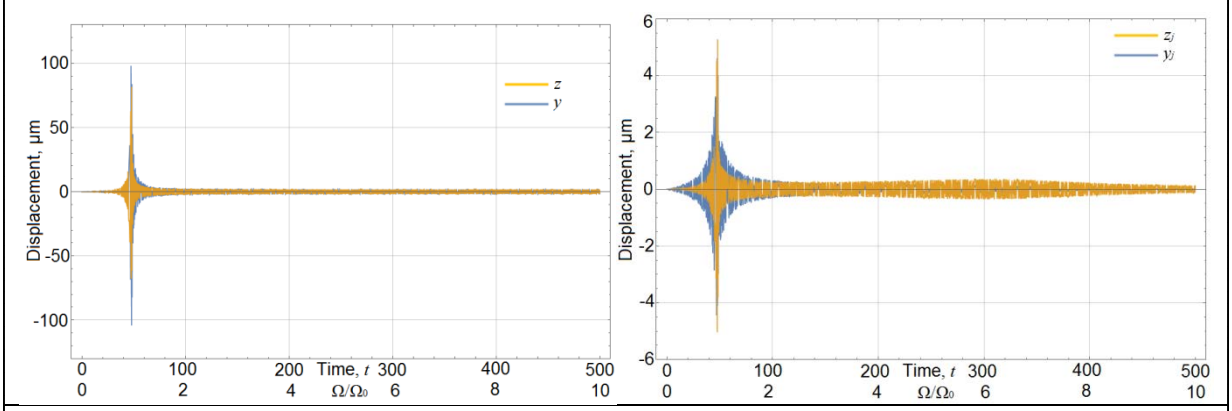

Figure 5. Disc (left) and journals (right) amplitude as a function of t (in sec.) and Ω; numerical solution

With $\Omega_0 = \sqrt{48EI / m_d / L^3}$ to be the 1st natural frequency of the Jeffcott rotor in rigid supports, see also table 1, the two of the eigenvalues of the system in equation (1) corresponding to rotating speed are evaluated as $\lambda_1 = 0.971\Omega_0$ and $\lambda_2 = 6.547\Omega_0$. The amplitude of disc and journal response as a function of rotating speed is plotted in figure 4 for the analytical solution and in figure 5 for the numerical solution using Runge-Kutta method. The 90μm amplitude of the disc and the 6μm amplitude of the journal response do correspond well to real applications. However, looking at the 1st critical speed peak at figures 4 and 5 it is seen that the amplification factor is very high in this frequency (or the effective damping is low) and that the 2nd critical speed is almost of negligible amplification factor. This will amplify the vibration reduction due to modal interaction and it is true that the real system under consideration experience much more effective damping at the 2nd critical

speed than at the 1st. The transient response is evaluated for $\Omega/\Omega_0 = 0 \sim 10$ and with low $\dot{\Omega}$ so as to obtain the highest resonance amplitude and to correspond also to real operation.

The numerical solution of equation (1) plotted in figure 5 will act as reference for the comparison of the numerically solved system when parametric excitation is introduced with the scheme presented in equations (3) and (4) [34]. The system, although linear, is not solved in this work using the classical Floquet theory for periodic elasticity effects and the numerical solution is preferred.

$$\begin{bmatrix} K_{YY}(t) & K_{YZ}(t) \\ K_{ZY}(t) & K_{ZZ}(t) \end{bmatrix} = \left(1+\varepsilon\sin\left(\Omega_{ex}t\right)\right)K\begin{bmatrix} 1.5 & -10 \\ -1 & 7 \end{bmatrix} \tag{3}$$

$$\begin{bmatrix} C_{YY}(t) & C_{YZ}(t) \\ C_{ZY}(t) & C_{ZZ}(t) \end{bmatrix} = \left(1+\varepsilon\sin\left(\Omega_{ex}t\right)\right)10^5\begin{bmatrix} 60 & -19 \\ -15 & 8 \end{bmatrix} \tag{4}$$

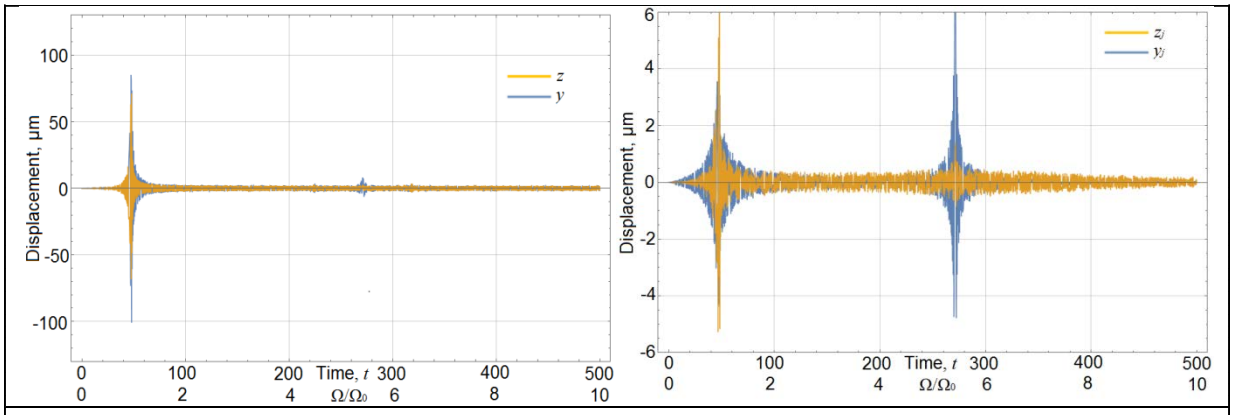

Figure 6. Stiffness and damping variation of $\varepsilon = 0.4$. Disc (left) and journals (right) amplitude as a function of t (in sec.) and Ω; numerical solution

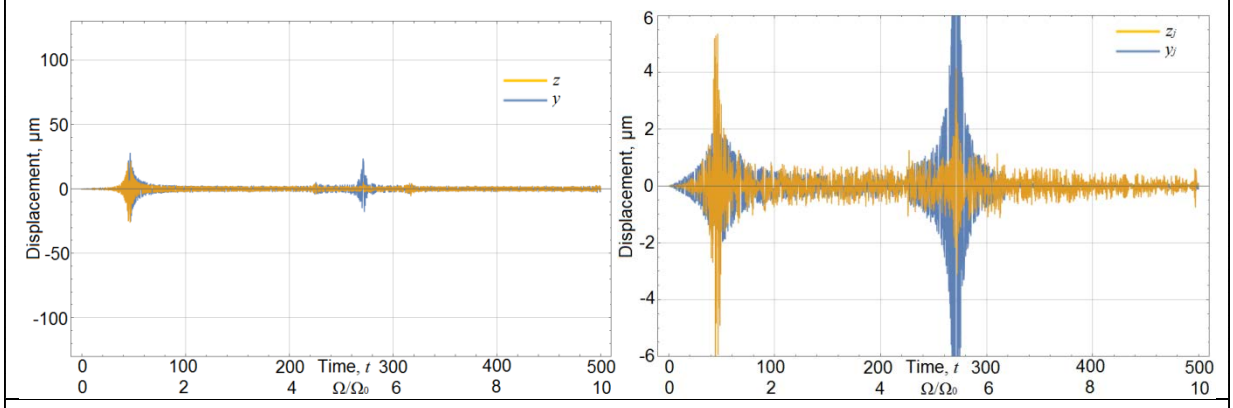

Figure 7. Stiffness and damping variation of $\varepsilon = 0.8$. Disc (left) and journals (right) amplitude as a function of t (in sec.) and Ω; numerical solution

The candidate values of Ω_{ex} that would introduce modal interaction in the system are $\Omega_{ex} = \left(\lambda_2 - \lambda_1\right)/n$ $(n \in \mathbb{Z}^*)$ if the system's stiffness and damping matrices are symmetrical, or $\Omega_{ex} = \left(\lambda_2 + \lambda_1\right)/n$ if the system's stiffness and damping matrices are not symmetrical [29-33]. In the current case the system's stiffness and damping matrices are symmetrical.

As it is shown in figure 6, a value of $\varepsilon = 0.4$ as amplitude of the stiffness and damping variation under an $\Omega_{ex} = 5.576\Omega_0$ would only create a resonance at rotating speed $\Omega = \Omega_{ex}$ at both disc and journals

without suppressing much the 1st critical speed amplitude. Increasing the variation further at $\varepsilon = 0.8$, the 1st critical speed amplitude is decreased at about 70% of its reference value shown in figure 5 while the journals would experience increased vibrations at $\Omega = \Omega_{ex}$; however, the amplification of response at such a frequency would not consist a problem since the operating range is supposed to be up to $3\Omega_0$.

4. Modal interaction and vibration suppression of turbine rotors

An example of applying modal interaction to an industrial steam turbine for power generation is presented in this section. The rotor model is implemented using the Transient Transfer Matrix Method (TTMM) [35] including additional masses of blading. Two bearings of variable geometry, see also figure 1 [27], of finite length are modelled as in [27] in order to introduce the parametric variation of their properties at the desired frequency and amplitude, as explained in section 3. The physical and geometric properties of the rotor-bearing system are presented in table 2 and a representation of the rotor outline is shown in figure 8.

Table 2. Basic geometrical and physical properties of the turbine rotor-bearing system

Rotor & Blades		Bearings		
			Bearing #1	Bearing #2
Total rotor mass	$M = 5500\text{kg}$	Load	$F_1 = 26\text{kN}$	$F_1 = 30\text{kN}$
Equivalent diameter	$D = 400\text{mm}$	Diameter	$D_1 = 180\text{mm}$	$D_2 = 200\text{mm}$
Mass polar moment	$J = 250\text{kgm}^2$	Length	$L_1 = 120\text{mm}$	$L_2 = 140\text{mm}$
Bearing span	$L = 3500\text{mm}$	Radial clearance	$c_1 = 180\mu\text{m}$	$c_2 = 200\mu\text{m}$
Young Modulus	$E = 210\text{GPa}$	Oil Viscosity	$\mu = 0.03\text{Pa}\cdot\text{s}$	$\mu = 0.03\text{Pa}\cdot\text{s}$

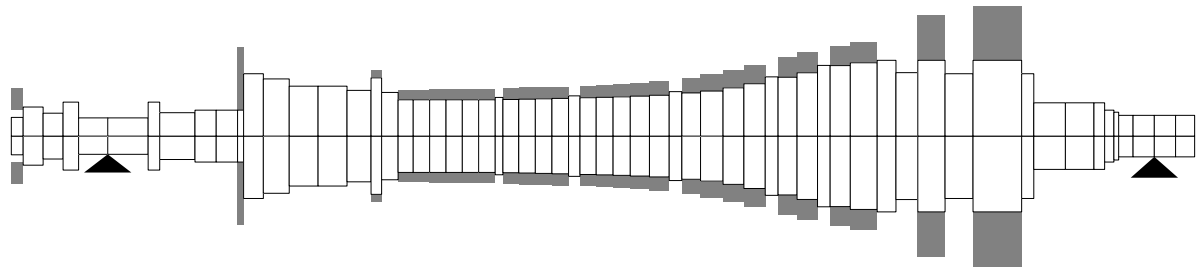

Figure 8. Approximate representation of the turbine used in this example and its discretization for the implementation of TTMM. Additional masses shown in dark, bearing locations indicated by triangle.

The TTMM is a method that combines the classical Transfer Matrix Method (Myklestad-Prohl method) with linear or nonlinear acting forces so as to perform linear or nonlinear transient response analysis [35]. The system is supposed to operate at a nominal speed of $\Omega = 700\text{rad/s}$ or $\Omega \approx 2.2\Omega_0$ where $\Omega_0 = 319.4\text{rad/s}$ is the first critical speed at the vertical direction. The discretization of the rotor consists of about 60 cylindrical rotor segments. The distributed total mass along each segment (shaft and blading) is represented by division to two equal concentrated masses at the ends of each segment. Each mass is supposed to execute its motion under the action of the shearing forces and moments of the sides segments including bearing forces and external forces (unbalance) when present. The response of each mass is evaluated in discrete time domain after the numerical solution of the segment's equations of motion that describe its motion.

The speed depended fluid film properties of stiffness and damping are evaluated for the theoretical range of operation $0<\Omega/\Omega_0<5$ and they are plotted in figure 9 for a specific range of Ω/Ω_0. The amplitude of periodic variation of the fluid film properties is represented in figure 9 for the K_{YY} and C_{YY} coefficient for an applied displacement of $\varepsilon=0.4$, see also eqs. (3) and (4). The sinusoidal variation shown in figure 9 is representative and does not correspond to the actual frequency of variation.

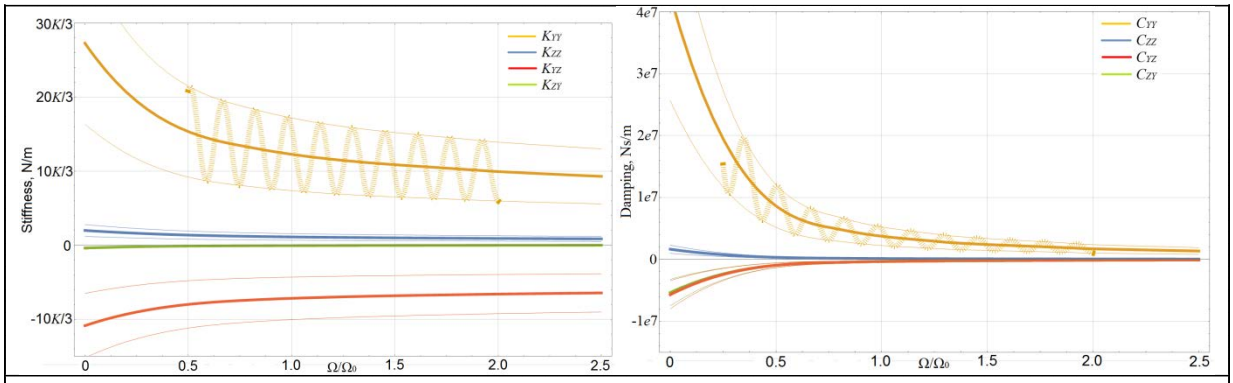

Figure 9. Speed depended stiffness (left) and damping (right) coefficients and their implemented amplitude of periodical variation, e.g $\varepsilon=0.4$.

The system executes a run-up at $0<\Omega/\Omega_0<5$ with a constant angular acceleration of $\dot{\Omega}=10\text{rad/s}^2$ or $\dot{\Omega}/\Omega_0^2\approx 9.8e-5$. The ratio of $\dot{\Omega}/\Omega_0^2\ll 1$ provides the minimum amplitude decrement due to transient phenomena during the passage through resonance. The unbalance magnitude complies to the standards for maximum permissible residual unbalance in steam turbines of higher speed. With the rotor to be mounted in conventional 2-arc journal bearings (see also figure 1) and without excitation, $\varepsilon=0$ and $\Omega_{ex}=0$, the system's response at mid-span and bearings is plotted in figure 10. In figure 10 it is shown that the system passes through the 1st critical speed with a relatively high amplification of the response in the vertical direction, while in horizontal direction the response appears well damped. The maximum amplitude in the operating range (0-rated speed) appears at the critical speed and is of about 440μm magnitude. Further increment of the rotating speed would decrease the rotor and journal response amplitude in horizontal and vertical direction, see figure 10 right. The system obtains the 2nd critical speed in the horizontal direction at about $\Omega/\Omega_0\approx 3.95$.

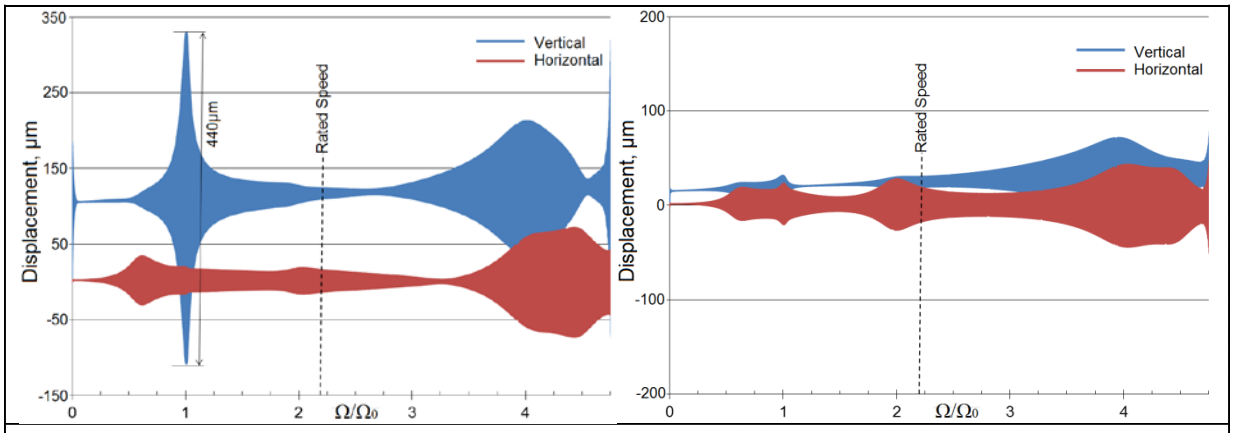

Figure 10. Unbalance response amplitude as a function of rotating speed at a constant run-up of the system without introducing parametric excitation; left: bearing mid-span, right: 1st bearing location

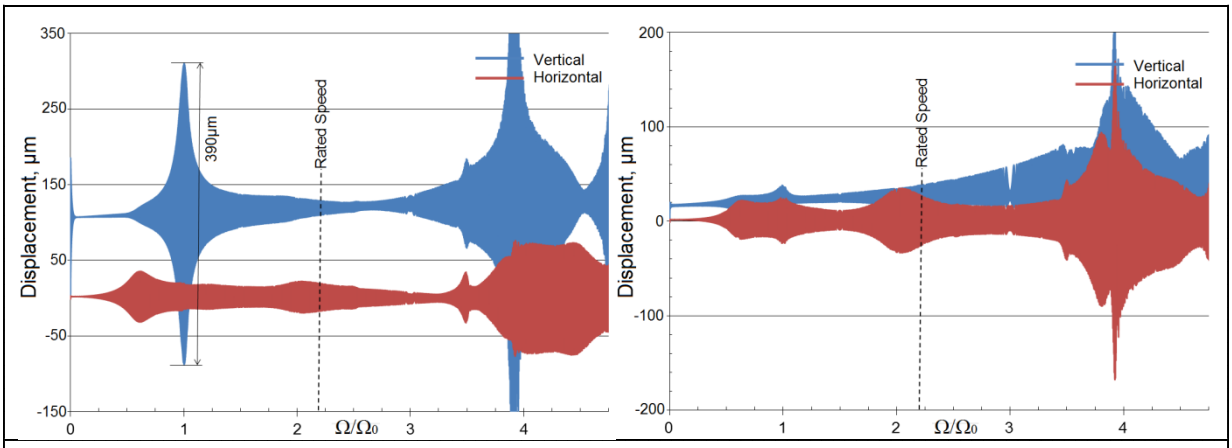

Figure 11. Unbalance response amplitude as a function of rotating speed at a constant run-up of the system introducing parametric excitation within $\varepsilon = 0.4$ and $\Omega_{ex} = 2.95\Omega_0$. Left: at the bearing mid-span; right: 1st bearing location

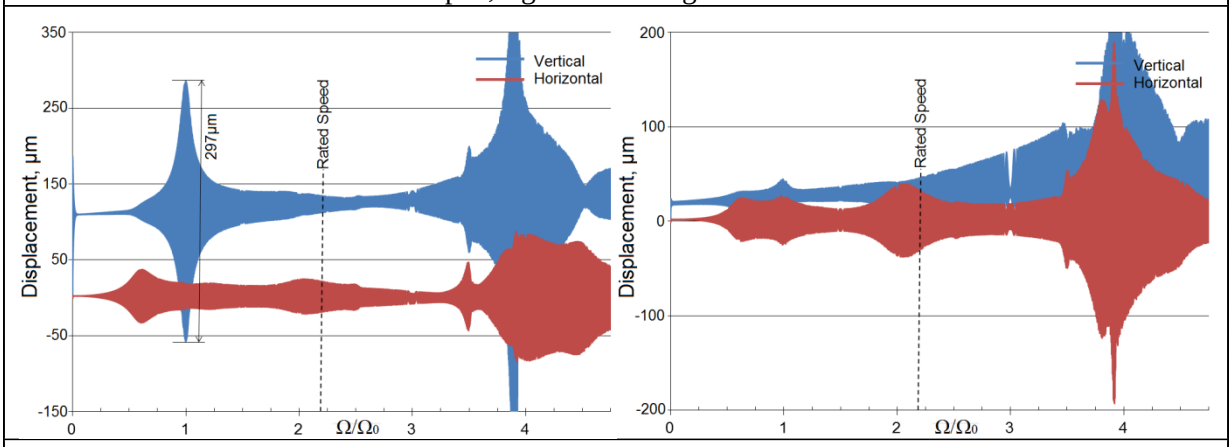

Figure 12. Unbalance response amplitude as a function of rotating speed at a constant run-up of the system introducing parametric excitation within $\varepsilon = 0.6$ and $\Omega_{ex} = 2.95\Omega_0$. Left: at the bearing mid-span; right: 1st bearing location

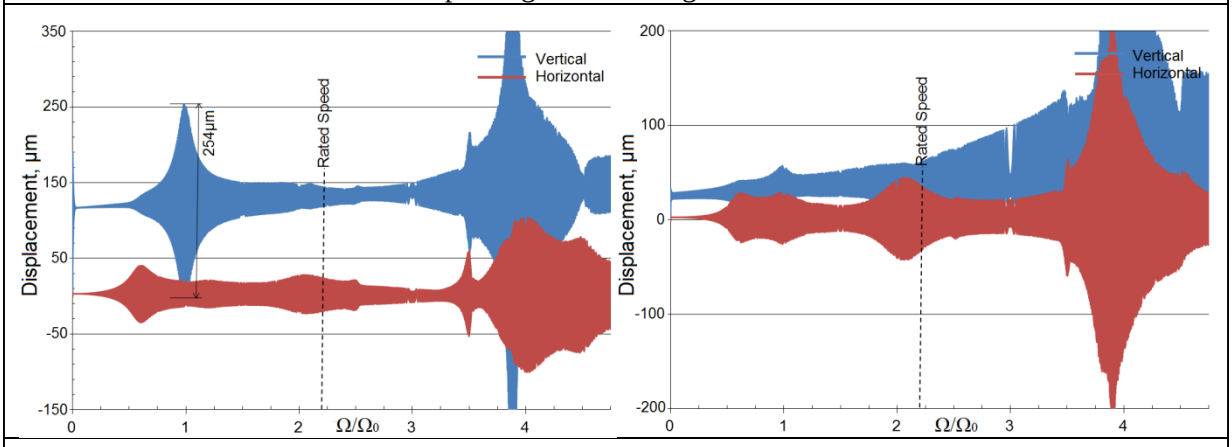

Figure 13. Unbalance response amplitude as a function of rotating speed at a constant run-up of the system introducing parametric excitation within $\varepsilon = 0.8$ and $\Omega_{ex} = 2.95\Omega_0$. Left: at the bearing mid-span; right: 1st bearing location

The journal bearings operate at a relatively low eccentricity when speed ratio is raised at higher values with the linear bearing coefficients to obtain such values that introduce instability. The bearing instability occurs in this application at a speed ratio $\Omega/\Omega_0 > 5$ and this corresponds to a relatively high speed. However, with the current bearing configuration of a loading sector of 50^o, the eccentricity of the bearings is relatively high and instability does not occur, even in higher speed ratios. Furthermore, the proposed bearing is supposed to enhance or even eliminate instability when parametric anti-resonance is introduced at the system [27, 33, 34]. However, one could notice that in the current example and with the bearings at 'non-excited' operation, instability will occur at $\Omega/\Omega_0 > 5$, see figure 10.

In continue, the parametric excitation is introduced at the system with the variation of the linearized stiffness and damping properties of the bearings at a dimensionless amplitude of $\varepsilon = 0.4$, see also eqs. (3) and (4). According to the description of section 3, a candidate frequency of excitation in which the modal interaction should occur is $\Omega_{ex} = (\lambda_2 - \lambda_1)/n$, where here $\lambda_1 = \Omega_0$ and $\lambda_2 = 3.95\Omega_0$ are the 1st and 2nd critical speed estimated from the response peaks; thus, an $\Omega_{ex} = 2.95\Omega_0$ is applied and the 1st and 2nd bending mode are supposed to get coupled, reducing the 1st critical speed amplitude form 440μm to 390μm as shown in figures 10 and 11 (left).

The modal coupling impacts the maximum amplitude developed during passage through resonances and at each critical speed transient vibrations of the corresponding mode are excited. Due to the mode coupling, if one mode is excited at a critical speed then energy is transferred to the other mode too. On one hand, the maximum amplitude at the first critical speed is decreased by modulation since some vibration energy is transferred to the highly damped second mode where it is partly dissipated. On the other hand, the maximum amplitude at the second critical speed is increased by modulation since some vibration energy is transferred to the lightly damped first mode. This sequence of events is better shown in figures 12 and 13 where bearing stiffness and damping variation is progressively increased at $\varepsilon = 0.6$ and $\varepsilon = 0.8$ respectively and the phenomenon of modal interaction is amplified.

A periodic modulation of the stiffness and damping properties can be decomposed to multiple harmonics (Fourier series). The weight/amplitude of the first harmonic is in general the dominant one. For a rotor, in general the lower modes possess low damping. Thus, it is anticipated that it is possible to find the two conditions "harmonic variation" and "low modal damping" in the same frequency range. For a complex system, higher modes can exist that have also low modal damping. In such a special case it depends whether the amplitude of the higher frequency modulation is large enough to be able to act as principal resonances for this specific mode or large enough to introduce a modal interaction of higher modes. Theoretically it is possible to have multiple modal interactions, however, in the systems analysed so far the lowest modes were the ones that dominated the interaction.

The result is decreased 1st critical amplitude and increased 2nd critical speed amplitude. However, the 2nd critical speed is out of the operational range in this example and in the most applications in such machines is avoided. The 1st critical speed amplitude reduction is at a range of 50%. The modal interaction has its major impact in amplitudes exactly at the frequencies of the coupling modes, the 1st vertical and the 2nd vertical critical speeds at this example.

The expected benefit of the vibration reduction considers the implementation of reduced rotor-stator clearances and the improved efficiency of the machine.

5. Conclusions

A journal bearing of adjustable geometry and properties is investigated in this paper on its potentiality to introduce modal interaction in a rotating system of simple and complicated geometry so as to reduce vibrations during the passage through resonance. The principle of applying parametric excitation in the system's properties of stiffness and damping was proved to establish a method for vibration suppression in turbomachinery. The application of the method in a simple Jeffcott rotor system and in

the more complicated steam turbine rotor encourages the further development of the concept with the critical speed amplitudes to be reduced up to 50%.

References

[1] Vance, J. M., and Li, J., 1996, ‘‘Test Results of a New Damper Seal for Vibration Reduction in Turbomachinery,’’ASME J. Eng. Gas Turbines Power, 118, pp. 843–846.
[2] San Andre´s, L., and Lubell, D., 1998, ‘‘Imbalance Response of a Test Rotor Supported on Squeeze Film Dampers,’’ ASME J. Eng. Gas Turbines Power, 120, pp. 397–404.
[3] El-Shafei, A., and Hathout, J. P., 1995, ‘‘Development and Control of HSFDs for Active Control of Rotor-Bearing Systems,’’ ASME J. Eng. Gas Turbines Power, 117, pp. 757–766.
[4] Forte, P., Paterno, M. and Rustighi, E., 2004, ‘A Magnetorheological Fluid Damper for Rotor Applications’, International Journal of Rotating Machinery, vol 10(3), pp. 175-182
[5] Carmignani, C., Forte, P. and Rustighi, E., 2006, Design of a novel magneto-rheological squeeze-film damper, Smart Materials and Structures, 15(1), pp. 164-170
[6] Zapomel, J., Ferfecki, P., and Forte, P., 2012, ‘A computational investigation of the transient response of an unbalanced rigid rotor flexibly supported and damped by short magnetorheological, squeeze film dampers’, Smart Material and Structures, 21, 105011
[7] Aravindhan T S and Gupta K 2006 Application of Magnetorheological Fluid Dampers to Rotor Vibration Control Advances in Vibration Engineering vol 5(4) pp 369-380
[8] Ulbrich H., and Althaus, J., 1989, ‘‘Actuator Design for Rotor Control,’’ 12th Biennial ASME Conference on Vibration and Noise, Montreal, Sept. 17–21, ASME, New York, pp. 17–22.
[9] Althaus J., Ulbrich H. and Jiger T., 1990. Active Chamber System for Control of Rotor Dynamics, Theory and Experiment, Proceedings of 3rd International Conference on Rotordynamics, Lyon, pp. 333-338.
[10] Althaus, J., Stelter, P., Feldkamp, B., and Adam, H., 1993, ‘‘Aktives hydraulisches Lager für eine Schneckenzentrifuge,’’ Schwingungen in rotierenden Machinen II, H. Irretier, R. Nordmann, and H. Springer, eds., Vieweg-Verlag, Braunschweig, Germany, 2, pp. 28–36.
[11] Santos, I. F., 1995, ‘‘On the Adjusting of the Dynamic coefficients of Tilting-Pad Journal Bearings,’’ STLE Tribol. Trans., 38 (3), pp. 700–706.
[12] Goodwin, M. J., Boroomand, T., and Hooke, C. J., 1989, ‘‘Variable Impedance Hydrodynamic Journal Bearings for Controlling Flexible Rotor Vibrations,’’ 12th Biennial ASME Conference on Vibration and Noise, Montreal, Sept. 17– 21, ASME, New York, pp. 261–267.
[13] Osman, T. A., Nada, G. S., and Safar, Z. S., 2001, ‘‘Static and Dynamic Characteristics of Magnetized Journal Bearings Lubricated With Ferrofluid,’’ Tribol. Int., 34(6), pp. 369–380.
[14] Santos, I. F., 1994, ‘‘Design and Evaluation of Two Types of Active Tilting- Pad Journal Bearings,’’ IUTAM Symposium on Active Control of Vibration, Bath, England, Kluwer, Dordreicht, The Netherlands, pp. 79–87.
[15] Santos, I. F., and Russo, F. H., 1998, ‘‘Tilting-Pad Journal Bearings with Electronic Radial Oil Injection,’’ ASME J. Tribol., 120, pp. 583–594.
[16] Santos, I. F., and Nicoletti, R., 1999, ‘‘THD Analysis in Tilting-Pad Journal Bearings Using Multiple Orifice Hybrid Lubrication,’’ ASME J. Tribol., 121, pp. 892–900.
[17] Santos, I. F., and Scalabrin, A., 2000, ‘‘Control System Design for Active Lubrication with Theoretical and Experimental Examples,’’ ASME Paper No. 2000-GT-643.
[18] Bently, D. E., Grant J. W., and Hanifan P., 1999, ‘‘Active Controlled Hydrostatic Bearings for a New Generation of Machines,’’ ASME Paper No. 2000-GT-354.
[19] Santos, I. F., and Nicoletti, R., 2001, ‘‘Influence of Orifice Distribution on the Thermal and Static Properties of Hybridly Lubricated Bearings,’’ Int. J. Solids Struct., 38(10–13), pp. 2069–2081.
[20] Nicoletti, R., and Santos, I. F., 2001, ‘‘Vibration Control of Rotating Machinery Using Active Tilting-Pad Bearings,’’ Proceedings of the IEEE/ASME International Conference on Advanced Intelligent Mechatronics, Como, Italy, July 8–11, pp. 589–594.
[21] Santos, I. F., Scalabrin A., and Nicoletti, R., 2001, ‘‘Ein Beitrag zur aktiven

Schmierungstheorie,'' Schwingungen in rotierenden Machinen VI, edited by H. Irretier, R. Nordmann, and H. Springer, eds., Vieweg-Verlag, Braunschweig, Germany, 5, pp. 21–30.
[22] J.K. Martin, D.W. Parkins, Testing of a large adjustable hydrodynamic journal bearing, Trib. Trans. STLE 44, 559-566 (2001).
[23] J.K. Martin, Improved performance of hydrodynamic bearings by proactive adjustment, Mecanique & Industries 12, 17-24 (2011).
[24] Bischof K.R., Zhou J., Analysis and measurement of a novel tight-tolerance tilt pad journal bearing design that provides increased stability in high speed turbomachinery. 2010 STLE Annual Meeting & Exhibition Conference, STLE-754827, Las Vegas, Nevada, USA, 16-20 May, 6 pages, (2010).
[25] Krodkiewski J. M., Sun L., 1995. Stability Control of Rotor-Bearing System by an Active Journal Bearing, Proc. of the International Conference on Vibration and Noise, Venice, pp. 217-225.
[26] J. M. Krodkiewski, Y. Cen and L. Sun, Improvement of Stability of Rotor System by Introducing a Hydraulic Damper into an Active Journal Bearing, International Journal of Rotating Machinery 1997, Vol. 3, No. 1, pp. 45-52
[27] Chasalevris A. and Dohnal F., Enhancing Stability of Industrial Turbines Using Adjustable Partial Arc Bearings. MOVIC & RASD 2016, University of Southampton, July 3-6, 2016
[28] Dohnal F., Suppressing self-excited vibrations by synchronous and time-periodic stiffness and damping variation, Journal of Sound and Vibration 306, pp. 136-152, 2007.
[29] Dohnal F., Damping by Parametric Stiffness Excitation – Resonance and Anti-Resonance, Journal of Vibration and Control 14, pp. 669-688, 2008.
[30] Dohnal F., General parametric stiffness excitation – anti-resonance frequency and symmetry, Acta Mechanica 196, pp. 15-31, 2008.
[31] Dohnal F., Parametric anti-resonance: theory, experiment and interpretation, Habilitation Thesis, TU Darmstadt, 2012.
[32] Dohnal, F. and Chasalevris, A. (2015), 'Inducing modal interaction during run-up of a magnetically supported rotor', 13th International Conference in Dynamical Systems Theory and Applications DSTA 2015.
[33] Dohnal, F., Pfau, B. and Chasalevris, A. (2015), 'Analytical predictions of a flexible rotor in journal bearings with adjustable geometry to suppress bearing induced instabilities', 13th International Conference in Dynamical Systems Theory and Applications DSTA 2015
[34] Pfau, B., Rieken, M. and Markert, R. (2015), 'Numerische Untersuchungen eines verstellbaren Gleitlagers zur Unterdruckung von Instabilitaten mittels Parameter-Antiresonanzen. 1st IFToMM D-A-CH Conference.
[35] Liew, A., Feng, N., and Hahn, E. (2004), 'On using the transfer matrix formulation for transient analysis of nonlinear rotor bearing systems', International journal of rotating machinery 10(6), pp. 425-431.